Open Access Online Journal on Astronomy and Astrophysics

Acta Astrophysica Taurica

www.astrophysicatauricum.org

Acta Astrophys. Tau. 5(4), 35–38 (2024)

Pre-impulsive flare energy release according to sub-terahertz and X-ray solar observations

V.V. Smirnova[1], Yu.T. Tsap[1], V.S. Ryzhov[2]

[1] Crimean Astrophysical Observatory, Nauchny
e-mail: vvsvid.smirnova@yandex.ru
[2] Bauman Moscow State Technical University, 2nd Baumanskaya str. 5, Moscow, 105005, Russia
e-mail: v_ryzhov@mail.ru

Received 22 October 2022

ABSTRACT

We study time delays between X-ray and sub-terahertz emission at the initial phase of solar flares to clarify the nature of heating of the transition region and upper chromosphere of the Sun. Analysis of a series of events showed that hard X-ray emission is delayed relative to sub-THz emission at the onset of flares by 3–6 minutes for some considered events. The electron thermal conductivity of the coronal plasma cannot ensure the effective heating of the transition region and solar chromosphere. This suggests the heating of the chromospheric plasma in situ during the pre-impulsive phase of solar flares.

Key words: Sun, solar flares, sub-terahertz radio emission, chromosphere

1 Introduction

The study of solar flare precursors in various wavelength ranges and on different time scales has always been of great interest (Charikov, 2000; Fleishman et al., 2022). In particular, Harrison et al. (1985) and Tappin (1991), using observations from the Solar Maximum Mission satellite, concluded that the growth of soft X-ray emission in the pre-impulsive phase of flares is characteristic of approximately half of all selected events. Meanwhile, information about the spatial location of emission sources remained unavailable for a long time due to the low resolution of instruments.

Relatively recently, thanks to high spatial resolution space observations with the Reuven Ramaty High Energy Solar Spectroscopic Imager (RHESSI) and Solar Dynamics Observatory (SDO), strong indications have appeared that X-ray sources before the impulsive phase of a flare can be located at the footpoints of coronal loops, and their temperature reaches 10–15 MK (Hudson et al., 2021). Since sub-terahertz (sub-THz) emission is closely related to X-ray one (Smirnova et al., 2021), and thermal plasma of the transition region and upper chromosphere can be responsible for its generation (Tsap et al., 2018; Kontar et al., 2018), one should expect a close relationship between sub-terahertz and X-ray data, including the microwave range (Altyntsev et al., 2012). The relevance of such studies becomes especially obvious if we take into account the importance of identifying the source of chromospheric plasma heating during the development of a flare, which may be associated with accelerated charged particles, thermal fluxes, and energy release in situ.

We aim to investigate the time delays between the profiles of X-ray and sub-THz emission observed before the impulsive phase of flares. Then, based on the results, we try to find out the nature of heating of the transition region and upper chromosphere of the Sun.

2 Observational data and selection of flare events

In this work, we used the results of observations of the sub-THz emission of solar flares obtained with the RT-7.5 radio telescope of the Bauman Moscow State Technical University, which monitors solar activity at frequencies of 93 and 140 GHz (Tsap et al., 2016). This unique instrument allows measuring the intensity of radio emission of solar flares with a spatial resolution of 2.5′ (93 GHz) and 1.5′ (140 GHz), with a time resolution of 1 s. Observations from the Solar Submillimeter Telescope (SST) in Argentina (Kaufmann et al., 2000) and the Köln Observatory for Submillimeter and Millimeter Astronomy (KOSMA, Lüthi et al., 2004) in Switzerland were also used. Data on the X-ray emission of flares were obtained using the RHESSI, Solar Orbiter (Spectrometer Telescope for Imaging X-rays instrument, STIX) and Fermi space observatories.

For the analysis of time profiles for delays between sub-THz and hard X-ray emission, we selected seven flares, four of which were observed with RT-7.5, two with SST, and one with KOSMA. These events are presented in the first column of Table 1. The second column indicates the X-ray class of

Table 1.

Date/Time (UT)	GOES class	Delays (min)	Frequency	Publication
SOL2001-04-12T10:28	X2.0	none	(230 GHz)	Lüthi et al. (2004)
SOL2006-12-06T18:47	X6.5	none	(212 GHz)	Kaufmann et al. (2009)
SOL2012-07-05T11:44	M6.1	none	(140 GHz)	Tsap et al. (2018)
SOL2013-02-17T15:50	*M1.9*	*2*	*(212 GHz)*	*Fernandes et al. (2017)*
SOL2017-04-02T07:50	M5.4	7	(140 GHz)	Morgachev et al. (2018)
SOL2022-03-28T11:26	M4.0	6	(93 GHz)	–
SOL2022-05-05T13:15	M2.2	3	(93 GHz)	–

the flare according to the data from the Geostationary Operational Environmental Satellite (GOES) near-Earth satellites. The events were selected in such a way that the signal-to-noise ratio in the sub-THz range was as good as possible, i.e., the constant noise component of the receiving equipment (excluding the background from the quiet Sun) did not exceed 10%. The level of the pre-flare background in the sub-THz and hard X-ray ranges was estimated using the local minimum close to the impulsive phase from observations at a frequency of 93 GHz and in the 25–50 keV channel according to the method given in Hudson et al. (2021). The error in determining the onset of the impulsive phase depends mainly on the signal-to-noise ratio and varies approximately from 1 to 5 s.

We compared time profiles of sub-THz and hard X-ray emission for delays prior to the onset of the energy release process. The duration of the delays in minutes is indicated in the third column of Table 1. The frequencies at which the observations were carried out, as well as the publications in which these events are described, are indicated in the fourth and fifth columns, respectively.

From Table 1 it can be seen that two X-class events and one M6.1-class event did not show visible delays, which is in good agreement with the standard model of solar flares. In four events, sub-THz emission preceded hard X-ray emission before the impulsive phase, and in one event (italicized in the table) a lag of the sub-THz emission profile relative to the X-ray one was observed. Thus, sub-THz emission did not precede hard X-ray emission for all flare events (see Table 1). On the one hand, this indicates the important role of flare precursors in the millimeter wavelength range, accompanied by chromospheric heating, and on the other hand, it suggests different phenomenology of flare energy release. In this regard, let us consider the SOL2022-03-28T10:58 event in more detail.

Observations at a frequency of 93 GHz were carried out by scanning the solar disk with a time resolution of 0.25 s. The time for one complete map of the solar disk to construct was six minutes. The maximum flux of sub-THz emission from the flare was determined by a detailed study of the moment the active region passed through the antenna beam for approximately 30 s. At the same time, an increase in the flux was recorded on the scans of the active region in the interval, which made it possible to reduce the error in determining the moment of the flare maximum emission to 30 s.

On the time profile (Fig. 1, left, panel [e]), asterisks indicate the moments for which the emission fluxes in the studied active region were obtained. In particular, it can be seen that at 11:14 UT, with an accuracy of ±30 s, the flux of sub-THz emission from the flare region already reaches ~10–20 s.f.u., while in the hard X-ray and microwave ranges, no significant flux increase occurs.

On the soft X-ray emission profiles, the rise phase of the flare, as well as on the sub-THz time profile, is observed for approximately 20 minutes (Fig. 1 left, panel [a]), which is a fairly common phenomenon (Smirnova et al., 2021). This additionally supports the correct estimation of the moment of the sub-THz emission maximum.

It is important to note that during the processing of the maps, the flux from the quiet Sun and the noise associated with the propagation of radio waves through the Earth's atmosphere were taken into account. The error in measuring the radio emission flux was ~25%, i.e., signal attenuation could not have a significant effect on the results obtained.

Figure 1 shows an example of the time profiles of the SOL2022-03-28T10:58 flare of GOES class M4.0, which occurred on March 28, 2022, in the active region 12975. The profiles of soft and hard X-ray emission in the channels from 1.5 to 84 keV were obtained from GOES [a] and STIX [b, c] data. Panel [d] shows the time profiles of the microwave radio emission of the flare at frequencies of 6 and 9 GHz, recorded by the telescopes of the Kislovodsk Mountain Station of the Pulkovo Observatory of the Russian Academy of Sciences. The time profile of radio emission at a frequency of 93 GHz is shown in panel [e]. The solid vertical line shows the time before the onset of the impulsive phase of the flare. The dashed line indicates the moment of the flare maximum according to observations at 93 GHz. It can be seen that at the maximum of the impulsive phase, the sub-THz emission lags behind the hard X-ray one by seven minutes. However, prior to the onset of the impulsive phase of the flare, the hard X-ray emission profile lags behind the sub-THz one by approximately six minutes.

Figure 2 shows a comparison of the X-ray emission profiles according to Fermi and GOES data. It can be seen that before the onset of the impulsive phase of the flare in soft X-ray emission, in the 4.5–15 keV channel, there is an increase in emission, whereas in the hard channels it remains at the noise level.

It can be assumed that the observed behavior of the profiles can be explained within the standard model of a solar flare by the fact that the heat transfer from the top of the flare loop to its footpoints occurred through thermal conduction, which led to the heating of the chromosphere emitting in the sub-THz range. In this case, the heating time of the chromospheric plasma should be comparable to the delays between

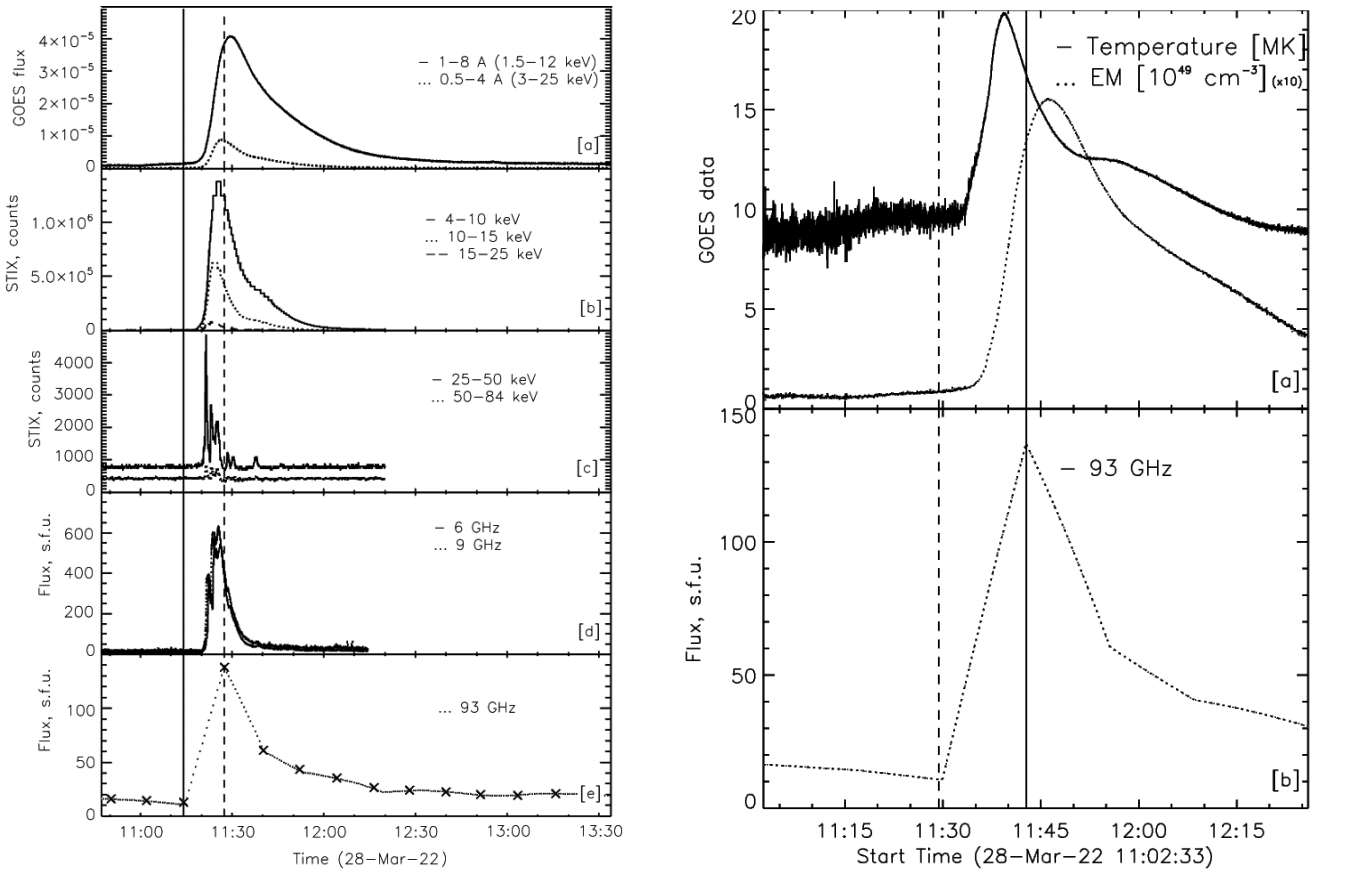

Fig. 1. Left: time profiles of the SOL2022-03-28T10:58 flare emission: soft X-rays in the 1.5–12 keV (GOES) and 4–25 keV (STIX) channels [a – b]; hard X-rays in the 25–50 and 50–84 keV (STIX) channels [c]; radio emission at frequencies of 6 and 9 GHz [d], and at a frequency of 93 GHz [e]. Right: profiles of the temperature distribution and emission measure according to GOES data [a] and the time profile at a frequency of 93 GHz [b].

the sub-THz and X-ray emission of the flare and be ~6 min. In this regard, let us make some estimates.

We estimate the power of energy release in the chromosphere due to electron thermal conductivity as follows (Priest, 1982):

$$q = \kappa \frac{d}{ds}\left(T^{5/2}\frac{dT}{ds}\right) = \kappa\frac{2}{7}\frac{d}{ds}\left(\frac{dT^{7/2}}{ds}\right) = \kappa\frac{2}{7}\frac{d^2T^{7/2}}{ds^2} \approx \kappa\frac{2}{7}\frac{T^{7/2}}{s^2},$$

where the thermal conductivity coefficient $\kappa = 10^{-6}$ erg $K^{-7/2}$ s^{-1}. Hence, assuming the thermal energy of the transition region and upper chromosphere $W_{th} = 3/2nkT$, where $k = 1.38 \times 10^{-16}$ erg/K is the Boltzmann constant, for the characteristic heating time of the transition region and upper chromosphere plasma of thickness $s = 3\times10^7$ cm at $n = 10^{11}$ cm^{-3} and $T = 10^5$ K, we find

$$\tau_{con} \approx \frac{W_{th}}{q} = 21\frac{kns^2}{\kappa T^{5/2}} \approx 10^5 \text{ s}.$$

The obtained estimate indicates an insignificant contribution of plasma thermal fluxes to the heating of the lower layers of the solar atmosphere. Considering the absence of microwave bursts in the pre-impulsive phase, this supports the important role of the heating of the chromospheric plasma in situ. At the same time, one should not rule out a significant contribution

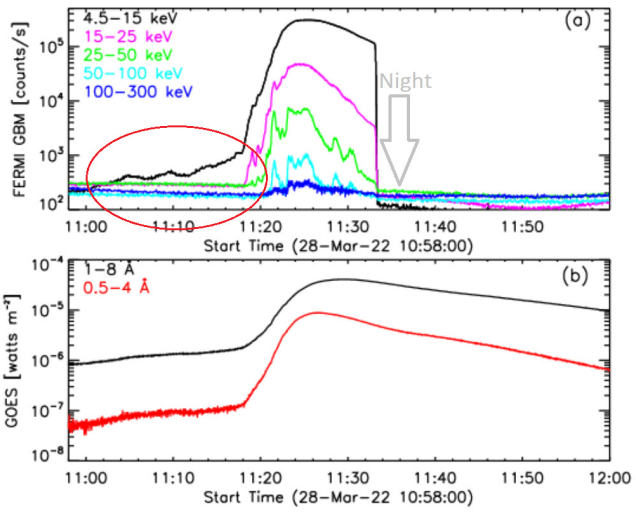

Fig. 2. Time profiles of the flare X-ray emission according to Fermi (a) and GOES (b) data.

of the "hot" (10^6–10^7 K) and dense X-ray plasma to sub-THz emission (Tsap et al., 2016).

3 Conclusions

Let us formulate the main results of the work.

1. Based on literature data and original observations, an analysis of a number of sub-terahertz events was carried out for the time delays between hard X-ray and sub-THz emission.
2. In three out of seven selected events, the onset of sub-THz emission generation precedes hard X-ray emission. This indicates that the heating of the chromospheric plasma in these flares is not associated with accelerated electrons.
3. Evidence has been obtained in favor of the important role of the thermal heating of the chromosphere in situ in the pre-impulsive phase of solar flares of X-ray class M.
4. Electron thermal conductivity of the coronal plasma cannot provide efficient heating of the transition region and chromosphere of the Sun during flare energy release.
5. Additional studies are needed since the coronal plasma can also make a significant contribution to the sub-THz emission of flares.

Acknowledgments. This work was supported by the RFBR grant No. 20-52-26006 Czech_a (V.V. Smirnova), the RSF grant No. 22-12-0030 (Yu.T. Tsap), and the Ministry of Education and Science research project No. 1021051101548-7-1.3.8 (Yu.T. Tsap, V.V. Smirnova).

References

Altyntsev A.A., Fleishman G.D., Lesovoi S.V., Meshalkina N.S., 2012. Astrophys. J., vol. 758, no. 2, p. 138.

Charikov Yu.E., 2000. Phys. Chem. Earth Part C: Solar, Terrestrial and Planetary Science, vol. 25, iss. 5–6, p. 407.

Fernandes L.O.T., Kaufmann P., Correia E., et al., 2017. Solar Phys., vol. 292, no. 1, p. 21.

Fleishman G.D., Martinez O.H.C., Landi E., Glesener L., 2022. Front. Astron. Space Sci., vol. 9, id. 966444.

Harrison R.A., Waggett P.W., Bentley R.D., et al., 1985. Solar Phys., vol. 97, iss. 2, pp. 387–400.

Hudson H.S., Simoes P.J.A., Fletcher L., Hayes L.A., Hannah I.G., 2021. Mon. Not. Roy. Astron. Soc., vol. 501, no. 1, pp. 1273–1281.

Kaufmann P., Trottet G., Giménez de Castro C.G., et al., 2000. Solar Phys., vol. 197, no. 2, pp. 361–374.

Kaufmann P., Trottet G., Giménez de Castro C.G., et al., 2009. Solar Phys., vol. 255, no. 1, pp.131–142.

Kontar E.P., Motorina G.G., Jeffrey N.L.S., et al. 2018. Astron. Astrophys., vol. 620, p. A95.

Lüthi T., Magun A., Miller M., 2004. Astron. Astrophys., vol. 415, pp. 1123–1132.

Morgachev A.S., Tsap Yu.T., Smirnova V.V., Motorina G.G., 2018. Geomagnetism and Aeronomy, vol. 58, no. 8, pp. 1113–1122.

Priest E.R., 1982. Solar Magnetohydrodynamics. Dordrecht: D. Riedel.

Smirnova V.V., Tsap Yu.T., Morgachev A.S., Motorina G.G., Bárta M., 2021. Geomagnetism and Aeronomy, vol. 61, no. 7, pp. 993–1000.

Tappin S.J., 1991. Astron. Astrophys. Suppl. Ser., vol. 87, no. 2, pp. 277–302.

Tsap Yu.T., Smirnova V.V., Morgachev A.S., et al., 2016. Adv. Space Res., vol. 57, iss. 7, pp. 1449–1455.

Tsap Yu.T., Smirnova V.V., Motorina G.G., et al., 2018. Solar Phys., vol. 293, no. 3, p. 50.